ACS Biomaterials SCIENCE & ENGINEERING

Article

pubs.acs.org/journal/abseba

Hydrogel-Coated Near Infrared Absorbing Nanoshells as Light-Responsive Drug Delivery Vehicles

Laura E. Strong and Jennifer L. West*

Department of Biomedical Engineering, Duke University, Durham, North Carolina 27708, United States

Supporting Information

ABSTRACT: Nanoparticle drug delivery carriers that can modulate drug release based on an exogenous signal, such as light, are of great interest, especially for improving cancer therapy. A light-activated delivery vehicle was fabricated by synthesizing a thin, thermally responsive poly(*N*-isopropylacrylamide-*co*-acrylamide) hydrogel coating directly onto the surfaces of individual near-infrared (NIR) absorbing gold-silica nanoshells. This hydrogel was designed to be in a swollen state under physiological conditions and expel large amounts of water, along with any entrapped drug, at elevated temperatures. The required temperature change can be achieved via NIR absorption by the nanoshell, allowing the hydrogel phase change to be triggered by light, which was observed by monitoring changes in particle sizes as water was expelled from the hydrogel network. The phase change was reversible and repeatable. As a model drug, the chemotherapeutic doxorubicin was loaded into this delivery vehicle, and rapid release of doxorubicin occurred upon NIR exposure. Further, colon carcinoma cells exposed to the irradiated platform displayed nearly 3 times as much doxorubicin uptake as cells exposed to nonirradiated particles or free drug, which in turn resulted in a higher loss of cell viability. We hypothesize these effects are because the NIR-mediated heating results in a transient increase in cell membrane permeability, thus aiding in cellular uptake of the drug.

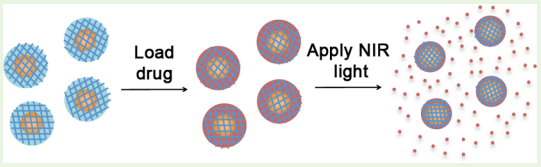

KEYWORDS: *optically triggered, thermally responsive, gold nanoshells, n-isopropylacrylamide, drug delivery, atom transfer radical polymerization (ATRP)*

1. INTRODUCTION

Near-infrared absorbing nanoparticles, particularly gold-based nanoparticles such as gold nanorods and gold−silica nanoshells, have been highly investigated for therapeutic treatment of cancer. This is due to numerous advantageous properties of the particles. First, the outer shell of these particles is made of reduced gold, a material known to be biocompatible because of its resistance to corrosion and low toxicity.[1−4] Second, the size of these particles (<500 nm) allows them to be injected intravenously and passively accumulate in tumor tissue because of the enhanced permeability and retention (EPR) effect related to the leakiness of tumor vasculature.[5] When these particles absorb near-infrared (NIR) light, which is highly tissue-penetrating and safe to normal tissues,[6,7] the electron-photon interactions within the gold shell yield to heat dissipation, resulting in photothermal ablation of nearby cells.[1,7−10]

By combining a near-infrared absorbing nanoparticle with thermally responsive hydrogels, which display sharp property changes in response to temperature changes, external control over polymer properties can be achieved through exposure to NIR light. Many thermally responsive hydrogels display lower critical solution temperature (LCST) behavior. At lower temperatures the polymeric material is in a highly hydrated state, but when transitioning to temperatures above the LCST, water moves into bulk solution and the polymeric material collapses onto itself forming hydrophobic interactions.[11−13] Therapeutic molecules may be absorbed into such a hydrogel and subsequently convectively released as water is expelled during the phase transition. Hydrogels with LCST behavior have been previously investigated in drug delivery applications.[14−16] The aim of this work is to synthesize such a material as a conformal coating on a nanoparticle as an injectable drug carrier with release activated by exposure to NIR light.

The particles utilized in these studies consist of a gold−silica nanoshell core, a 150 nm NIR absorbing nanoparticle that has been widely investigated for photothermal ablation of cancer,[17] with a ∼90 nm poly[*N*-isopropylacrylamide-*co*-acrylamide] (NIPAAm-*co*-AAm) hydrogel coating. The NIPAAM-*co*-AAm formulation is designed to have an LCST from 39 to 45 °C, so as to be in a swollen state under physiological temperatures, and transition to a collapsed state upon heating induced by NIR irradiation.[16] The poly(NIPAAm-*co*-AAm) coating was synthesized using surface initiated-atom transfer radical polymerization (SI-ATRP), a technique that tightly limits free radical generation to only the site of an initiator molecule.[18]

2. EXPERIMENTAL SECTION

2.1. Materials. All reagents were purchased from Sigma-Aldrich and used as received, unless otherwise noted. Prior to use, *N*-isopropylacrylamide (NIPAAm, 97%) was dissolved in tetrahydrofuran (THF) and recrystallized in *n*-hexane to remove the small molecule

Received: March 4, 2015
Accepted: June 10, 2015
Published: June 10, 2015

DOI: 10.1021/acsbiomaterials.5b00111
ACS Biomater. Sci. Eng. 2015, 1, 685−692

inhibitor *p*-methoxyphenol from the packaged NIPAAm. The recrystallization process was repeated at least 3 times and the final product was dried under vacuum and stored at −20 °C.

2.2. Fabrication of Hydrogel-Coated Particles. Gold−silica nanoshells were synthesized using previously described methods.[19] A 50 mL solution containing 1.5 wt % sodium alginate and nanoshells at an O.D. of 2 (5.8×10^9 nanoshells/ml) was prepared in H_2O. This solution was then added dropwise to 100 mL of 1 wt % $CaCl_2$ in H_2O under rapid stirring. This resulted in the formation of many small Ca^{2+}−alginate−nanoshell hydrogel "beads". The reaction mixture was stirred for 15 min, after which the Ca^{2+}−alginate−nanoshell "beads" were collected by filtration and rinsed 3 times with H_2O.

Next, the initiator bis[2-(2′bromoisobutryloxy)ethyl]disulfide (subsequently referred to as Br-initiator; ATRP solutions, Pittsburgh, PA) was immobilized onto the surface of the gold-silica nanoshells via gold−thiol interactions. First, a 50 mL solution containing 20 mM Br-initiator and 10 mM tris(2-carboxyethyl)phosphine (TCEP) (Thermo Fisher Scientific) in 1:1 EtOH:H_2O was incubated at RT for 60 min. This step serves to reduce the disulfide bond in the Br-initiator, resulting in two molecules with terminal thiol groups that can then assemble onto the gold-silica nanoshells through gold−thiol interactions. For immobilization onto the gold−nanoshell surface, the Ca^{2+}−alginate−nanoshell hydrogels were soaked in this Br-initiator/TCEP solution and rocked overnight at 4 °C. The next day, the gels were washed 3 times with EtOH followed by 3 times with H_2O to remove any nonimmobilized molecules.

The Ca^{2+}-alginate hydrogels containing the Br-initiator immobilized nanoshells were soaked in a 100 mL solution of 98:2 MeOH:H_2O (v/v) in a three-neck round-bottom flask. Under rapid stirring, the flask was evacuated and Ar gas was bubbled through the solution for 30 min to remove dissolved O_2. After 30 min, the following ATRP reaction components were added to the flask to the following concentrations: NIPAAm (23.75 mM), acrylamide (1.25 mM), methylene bis-(acrylamide) (0.0333 mM), CuBr (0.2 mM), 2,2′-bipyridine (0.6 mM), and $CuBr_2$ (0.02 mM). The flask was again evacuated and Ar was bubbled for an additional 30 min. The reaction mixture was then stirred at 1000 rpm for 18 h, after which the reaction was stopped by opening the flask to air.

The Ca^{2+}−alginate hydrogels were collected by filtration, and then rinsed 5 times with MeOH followed by 5 rinses with H_2O to remove any unreacted components. The Ca^{2+}−alginate−nanoshell beads were then soaked in 50 mL of 100 mM EDTA in TRIS buffered saline (TBS). This solution was vortexed for 1 min and then rocked at RT for 30 min to allow for sufficient chelation of the Ca^{2+} ions and dissolution of the Ca^{2+}−alginate hydrogels. The hydrogel-coated particles were then collected via 2 rounds of centrifugation (735*g*, 15 min) and the solution was passed through a 5 μm polycarbonate membrane filter.

2.3. Characterization of Hydrogel-Coated Nanoshells. Bare nanoshells, initiator-functionalized nanoshells, and hydrogel-coated nanoshells were characterized using UV−vis spectroscopy, DLS, zeta potential analysis, and TEM. Extinction spectra from 400 to 1000 nm were collected using a Cary 50 Varian spectrophotometer. DLS and zeta potential were measured using a Malvern Zetasizer Nano ZS. An FEI Tecnai G^2 Twin was used for TEM imaging. For analysis of particle stability, bare nanoshells and hydrogel-coated nanoshells were each suspended in 100 mM NaCl, and a UV−vis spectrometer (Cary 50 Bio, Varian) was used to record the particle spectra every 60 min over 4 h. Stability was calculated for each time point by expressing the peak extinction at that time point as a percent of the peak extinction of that sample at t = 0 min.

2.4. Thermal Deswelling. DLS measurements were used to investigate changes in particle size in response to increased temperatures as well as NIR irradiation. Measurements were taken at increasing temperatures (25, 37, and 60 °C) as well as after particles were exposed to NIR irradiation (Coherent Diode, 808 nm, 4 W/cm^2, 2 min). Temperatures were maintained for at least 15 min before a reading was taken. Z-average hydrodynamic diameters of all groups were compared using an ANOVA with Tukey's HSD (*p < 0.05). Additionally, particles were exposed to cyclic NIR irradiation (Coherent Diode, 808 nm, 4 W/cm^2, 3 min) followed by 10 min without irradiation for three cycles, with *Z*-average hydrodynamic diameters being reported.

2.5. Doxorubicin Loading and Release. For loading, the hydrogel-coated nanoshells were first pelleted by centrifugation (735*g*, 15 min) and suspended in a 2 mg/mL solution of doxorubicin in TBS. This suspension was then rocked at 4 °C for 72 h to allow for sufficient loading of the doxorubicin into the particles. After 72 h, we purified doxorubicin-loaded hydrogel-coated nanoshells by 3 rounds of centrifugation (735*g*, 15 min). The amount of doxorubicin loaded into the particles was determined using UV−vis spectroscopy (see the Supporting Information).

For release studies, doxorubicin-loaded hydrogel-coated nanoshells were suspended in TBS at an optical density (OD) of 0.5 (1.2×10^9 particles/mL). 500 μL aliquots of this suspension were either (1) exposed to an NIR laser (Coherent, 808 nm, 4 W/cm^2) for 3 min, (2) left at room temperature for 3 min, or (3) left at room temperature for 72 h, with each condition tested in triplicate. After exposure, the suspension was filtered through a 0.22 μm poly(ether sulfone) membrane (Genesee Scientific) to separate the doxorubicin-loaded hydrogel-coated nanoshells from the free doxorubicin in the sample. Doxorubicin content of the samples was then determined by measuring absorbance at 485 nm. The amounts of doxorubicin delivered under the three conditions were analyzed by an ANOVA with a Tukey's HSD. A similar setup was used when analyzing doxorubicin release in response to cyclic NIR exposure, with a 1.2 mL suspension of particles in TBS being exposed to NIR irradiation in a cycle of 3 min on, 3 min off, and 3 min on. At each time point, 0.4 mL of the suspension was removed and assayed for delivered doxorubicin content.

2.6. Drug Delivery to Carcinoma Cells. Murine colon carcinoma cells (CT-26.WT cells, ATCC) were cultured in RPMI 1640 media (ATCC) supplemented with 2 mM L-glutamine, 10 mM HEPES, 1 mM sodium pyruvate, 4.5 g/L glucose, 1.5 g/L sodium bicarbonate, 100 U/L penicillin, 100 mg/mL streptomycin, and 10% FBS (Atlanta Biologicals). Cultures were maintained at 37 °C with 5% CO_2. Cells were seeded at a density of 4000 cells/well in fibronectin-coated 96-well plates. Cells were allowed to adhere overnight before particle dosing, and each experimental group was assessed in triplicate.

Cells were exposed to five different conditions: (1) hydrogel-coated nanoshells loaded with doxorubicin, exposed to NIR irradiation, (2) hydrogel-coated nanoshells loaded with doxorubicin (no irradiation), (3) hydrogel-coated nanoshells (no doxorubicin) exposed to NIR irradiation (to evaluate photothermal effects), (4) 29 μg/mL free doxorubicin (~50 nM, equivalent to the amount of doxorubicin loaded in the particles in groups 1 and 2), or (5) no treatment. Particles were added to the cells at an OD of 0.25 (6×10^7 particles/well, or ~15,000 particles/cell) and incubated for 30 min prior to irradiation. For all cases exposed to NIR irradiation, cells were irradiated at 808 nm at 4 W/cm^2 for 3 min (beam size of 0.8 cm^2, total energy delivered was 720 J/cm^2). Cells were further incubated in the presence of the particles for an additional 24 h.

At 24 h post particle dosing, cellular uptake of doxorubicin was assayed by fluorescent microscopy (560 nm excitation, 645 nm emission) using an Axiovert 135 inverted fluorescent microscope (Zeiss). Doxorubicin fluorescent intensity was quantified using ImageJ (NIH) and analyzed using a Student's t test.

At 24 h post particle dosing, cell viability was assessed using an MTS assay. Media in each well was removed and fresh media with MTS reagent (CellTiter 96 AQueous One, Promega) was added (100 μL media/20 μL reagent per well). After a 60 min incubation at 37 °C and 5% CO_2, absorbance readings of the media were taken at 490 nm. Absorbance readings were normalized to readings of the cell-only control (Group 5) and compared using an ANOVA with a Tukey's HSD.

3. RESULTS

3.1. Fabrication of Hydrogel-Coated Particles. Figure 1A outlines the current synthesis process. First, gold−silica

DOI: 10.1021/acsbiomaterials.5b00111
ACS Biomater. Sci. Eng. 2015, 1, 685−692

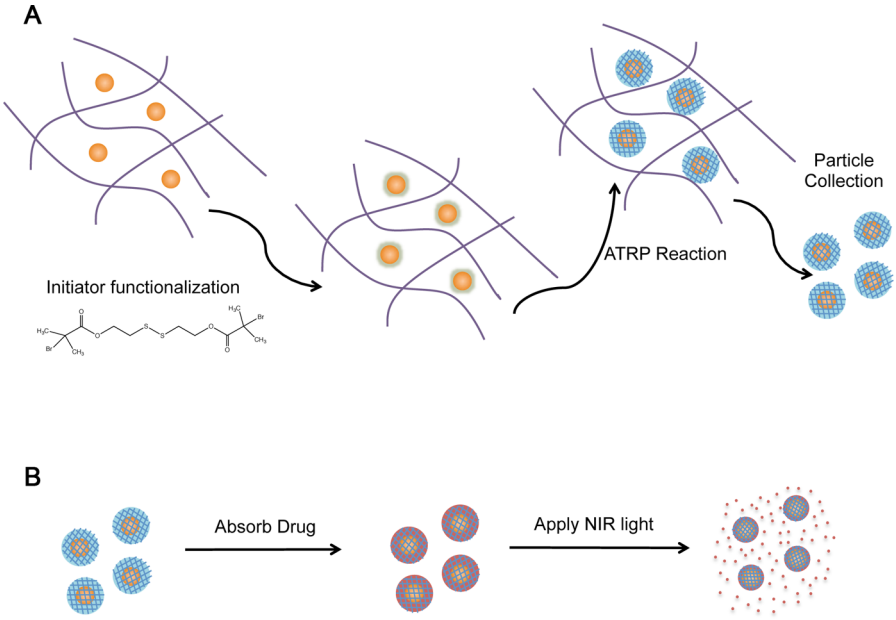

Figure 1. Schematics of (A) particle synthesis and (B) drug release. (A) (1) Nanoshells are encapsulated in Ca^{2+}-alginate hydrogel. (2) Ca^{2+}-alginate-nanoshell composite hydrogels are soaked overnight in a solution of the disulfide-containing ATRP initiator molecule to allow for assembly onto the nanoshell surface via gold−thiol interactions. (3) Ca^{2+}-alginate-initiator functionalized nanoshell composites are reacted in an ATRP solution with monomers, cross-linker, and catalyst molecules for 18 h. (4) Calcium chelating agent (EDTA) is added for dissolution of Ca^{2+}-alginate hydrogels and poly(NIPAAm-*co*-AAm) -coated nanoshells are collected. (B) (1) Poly(NIPAAm-*co*-AAm)-coated nanoshells are soaked in a drug solution (e.g., doxorubicin, MW 580 Da) for 3 days. (3) Particles are purified from drug solution by centrifugation. (2) NIR laser applied to drug-loaded particles causing localized heating of the embedded gold nanoshell, which in turn causes collapse of the thermally responsive poly(NIPAAm-*co*-AAm) hydrogel coating and a burst release of the loaded drug molecules.

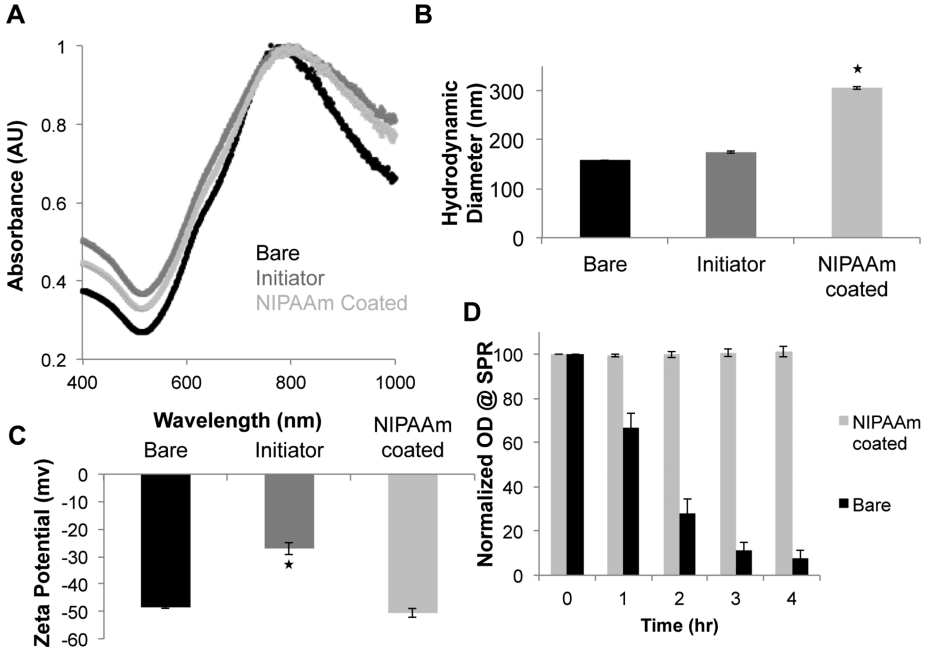

Figure 2. Characterization of bare, initiator-functionalized, and NIPAAm-coated nanoshells. (A) Extinction spectra shows that bare nanoshells have a peak extinction in the NIR at 785 nm. The spectra did not change significantly for the initiator-functionalized and NIPAAm-coated nanoshells, with only a slight peak broadening toward the red. (B) DLS measurements shows the hydrodynamic diameter of the particles increased from ∼159 nm for bare nanoshells to ∼188 nm for initiator-functionalized nanoshells to ∼337 nm for NIPAAm-coated nanoshells. (C) Zeta potential measurements show a more positive charge for initiator-functionalized nanoshells than the bare or hydrogel-coated nanoshells. (D) Changes in peak extinction of bare and poly(NIPAAm-*co*-AAm)-coated nanoshells over a 4 h suspension in 100 mM NaCl. The poly(NIPAAm-*co*-AAm)-coated nanoshells remained stable over the 4 h period as determined by minimal changes in their extinction spectra, whereas bare nanoshells aggregated and crashed out of solution over time. (*p < 0.01, ANOVA).

nanoshells were encapsulated in a Ca^{2+}−alginate matrix, which acted to prevent particle aggregation during the synthesis process. This matrix was designed to allow for very facile collection of the final particles since the alginate rapidly

DOI: 10.1021/acsbiomaterials.5b00111
ACS Biomater. Sci. Eng. 2015, 1, 685−692

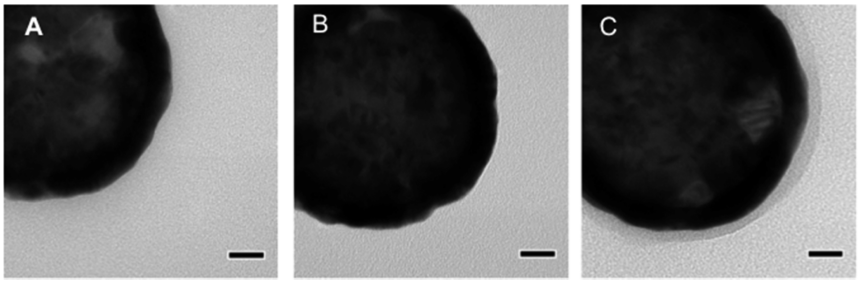

Figure 3. TEM images of (A) bare, (B) initiator functionalized, and (C) hydrogel-coated nanoshells. Bare and initiator-functionalized nanoshells look similar as the initiator molecule is too small to be visible. Hydrogel-coated nanoshells display a thin polymer coating around the electron dense gold nanoshell. Scale bars = 20 nm.

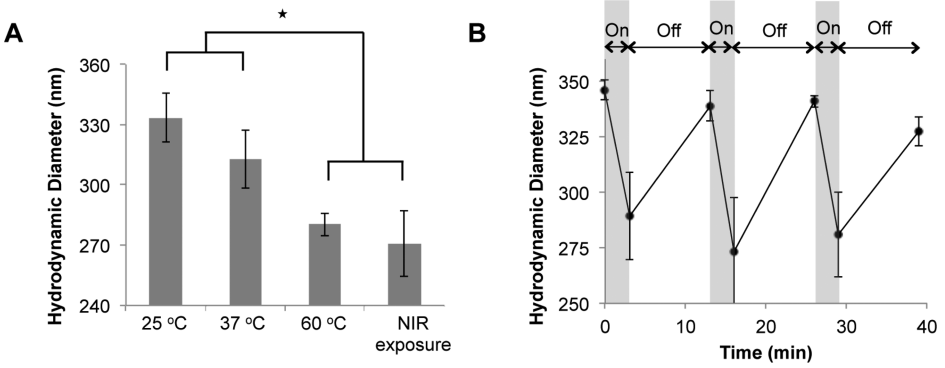

Figure 4. Thermal deswelling characterization. (A) Hydrodynamic diameters of particles at 25, 37, and 60 °C, and after exposure to NIR irradiation. Particles at 25 and 37 °C are not significantly different in size, but are both significantly larger than particles exposed to NIR irradiation or at temperatures above the material LCST (60 °C) (*p < 0.01, ANOVA). (B) Changes in particle diameter in response to cyclic NIR irradiation. Particles were exposed to NIR irradiation for 3 min followed by 10 min without NIR exposure for 3 cycles.

dissolves upon calcium chelation. Next, a thiol-containing initiator molecule was bound to the gold nanoshell surfaces. The poly(NIPAAm-*co*-AAm) hydrogel coating was then synthesized by adding the NIPAAm and AAm monomers, methylenebis(acrylamide) (MBAAm) as a cross-linker, and CuBr as an ATRP catalyst. After coating growth was complete, the Ca^{2+}−alginate matrix was dissolved by the addition of the calcium chelating agent EDTA, and the coated nanoparticles were collected. Figure 1B describes the loading and light-triggered release of drugs.

3.2. Characterization of Hydrogel-Coated Particles. The extinction spectra of bare nanoshells, initiator-functionalized nanoshells, and hydrogel-coated nanoshells are shown in Figure 2A. Bare nanoshells were found to have peak extinction at approximately 785 nm. This spectrum did not change significantly for the initiator-functionalized and hydrogel-coated nanoshells. Bare, initiator-functionalized, and hydrogel-coated nanoshells were analyzed using both DLS and zeta potential measurements (Figure 2B,C). A slight increase in hydrodynamic diameter was observed between the bare and initiator-functionalized nanoshells (158.6 nm vs 187.8 nm), with a much larger size seen for the hydrogel-coated nanoshells (337.4 nm, Figure 1B). An increase in surface charge was observed when functionalizing the nanoshells with the Br-initiator molecule (−48.5 mV for bare nanoshells vs −27.0 mV for initiator-functionalized nanoshells), but addition of the hydrogel coating shielded the initiator and returned the particles to a more negative state, as shown in Figure 2C.

In previous studies utilizing gold−silica nanoshells for photothermal therapies, the particle surface has been passivated by the attachment of PEG-thiol.[9] This coating serves several purposes, including preventing the nanoparticles from aggregating in the presence of physiological salt concentrations. Additionally, when these particles are injected in vivo this coating serves to minimize plasma protein adsorption and subsequent RES clearance. To analyze whether the poly(NIPAAm-*co*-AAm) hydrogel coating acts in a similar manner, we analyzed solution stability of bare nanoshells and hydrogel-coated particles exposed to 100 mM NaCl. Spectra of the hydrogel-coated particles did not change significantly over time, with absorption values (785 nm) maintaining over 95% of their original value over the 4 h time period. The bare nanoshells, however, very quickly aggregated in the high salt environment and began to fall out of solution (Figure 1D).

Particle cytotoxicity was analyzed in cells exposed to hydrogel-coated nanoshells using an MTS assay, an established method for determining nanoparticle toxicity.[20] Cytotoxicity was analyzed against two different cell lines: mouse embryonic fibroblasts (NIH 3T3s), a generic cell line commonly used in many cytotoxicity assays, and human hepatocarcinoma cells (HepG2s), as these cells have similar responses to hepatocytes and liver uptake of these particles is expected when used in vivo.[20] Hydrogel-coated nanoshells did not exhibit any material cytotoxicity against either the fibroblasts or hepatic cells (see the Supporting Information).

Figure 3 shows TEM images of bare nanoshells, initiator-functionalized nanoshells, and hydrogel-coated nanoshells. Both the bare and initiator-functionalized nanoshells look very similar, as the initiator molecule is too small to be visible. However, the hydrogel-coated particles display a thin polymer coating around the electron dense gold nanoshell. These images were taken under vacuum, and therefore the hydrogel

DOI: 10.1021/acsbiomaterials.5b00111
ACS Biomater. Sci. Eng. 2015, 1, 685−692

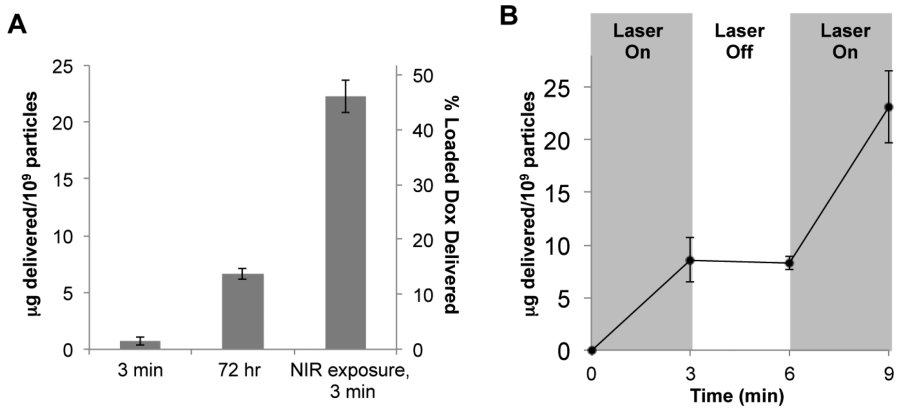

Figure 5. Delivery of doxorubicin from hydrogel-coated nanoshells. (A) After only 3 min of NIR irradiation, approximately 46% of the loaded doxorubicin is released from the particles. Release due to diffusion at room temperature is minimal, with less than 15% of the payload released over 72 h. (B) Doxorubicin-loaded hydrogel-coated nanoshells exposed to cyclic NIR irradiation (3 min on, 3 min off, 3 min on) demonstrate that doxorubicin is primarily released only when the NIR laser is on, with negligible release seen when the NIR laser is off.

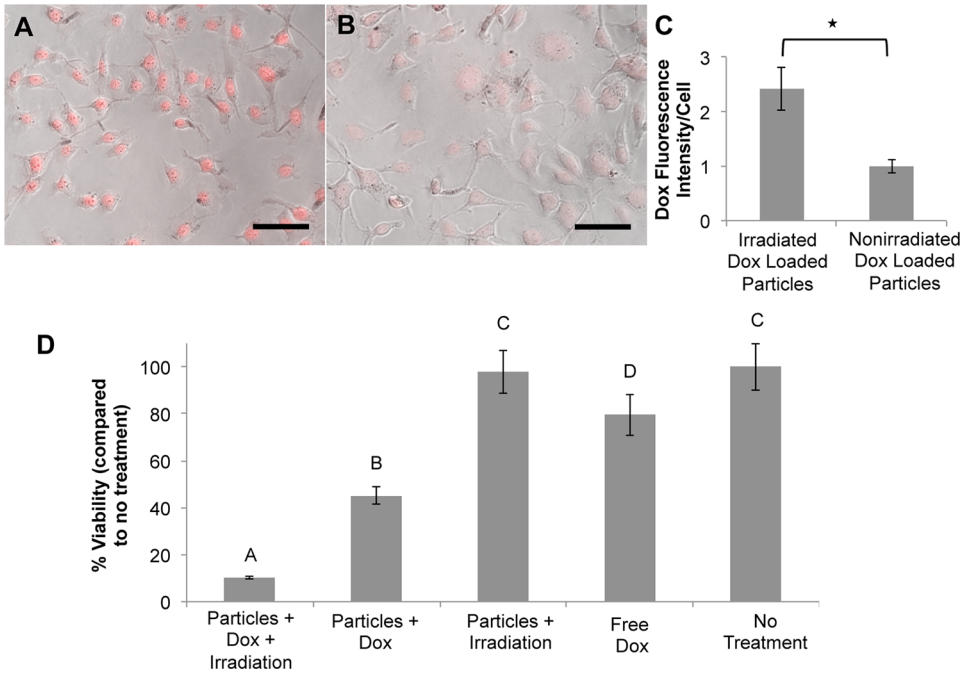

Figure 6. Uptake of doxorubicin by CT.26WT cells. Phase contrast images overlaid with doxorubicin fluorescent signal for cells exposed to (A) irradiated doxorubicin-loaded hydrogel-coated nanoshells or (B) nonirradiated doxorubicin-loaded hydrogel-coated nanoshells. Scale bars = 100 μm. (C) Quantification of doxorubicin fluorescence intensity per cell. Cells exposed to the irradiated drug-loaded particles showed almost 2.5× more doxorubicin fluorescence than cells exposed to nonirradiated drug loaded particles (*$p < 0.001$, Student's t test). (D) Changes in cell viability due to various treatment groups. Groups not connected by the same letter are statistically different from each other (*$p < 0.05$, ANOVA). Cells exposed to drug-loaded particles triggered to release their doxorubicin payload by NIR irradiation showed increased loss in cell viability compared to cells exposed to drug-loaded particles not exposed to NIR irradiation.

layer was fully dehydrated, leading the hydrogel coating to appear much thinner than it did when assessed in a hydrated state via DLS analysis.

3.3. Thermal Deswelling. The influence of temperature on particle size was investigated using DLS (see the Supporting Information). Hydrogel-coated particle sizes ranged from ~326 nm at 25 °C to ~280 nm after incubation at 60 °C, indicating that the hydrogel coating on the nanoshells transitioned from a hydrated to a collapsed state at a temperature above the LCST (Figure 4A). No significant size differences were seen between particles incubated at 25 or 37 °C, indicating the particles will be in their swollen state under physiological conditions. Hydrogel-coated particles exposed to NIR light were smaller (~270 nm) than the particles at 25 or 37 °C, and similar to the particles at 60 °C, indicating these particles have undergone the phase transition, expelling water from the poly(NIPAAm-*co*-AAm) coating (Figure 4A). Additionally, the particles can effectively cycle between their swollen and collapsed states when exposed to cyclic NIR exposure (3 min on, 10 min off) (Figure 4B). Particle diameters decrease in response to the NIR irradiation, and increase back to their original size within 10 min of the NIR laser being turned off.

3.4. Drug Loading and Release. Doxorubicin was used as a model drug for these studies both due to its importance in cancer therapy and because its optical properties facilitate studies of drug loading, release and uptake in cells. Doxorubicin

DOI: 10.1021/acsbiomaterials.5b00111
ACS Biomater. Sci. Eng. 2015, 1, 685−692

loading into the hydrogel-coated nanoshells was assessed using UV−vis spectroscopy (see the Supporting Information). Overall, 48.4 ± 0.3 μg of doxorubicin was loaded per 10^9 particles, equating to approximately 5×10^7 doxorubicin molecules per particle. On the basis of these loading levels, ~3.12×10^9 particles would be needed to achieve the maximum tolerated dose of free doxorubicin in mice (5 mg/kg).[21] This particle concentration is well below gold-silica nanoshell doses that have been previously used in mice (~1×10^{11} particles/mouse),[9] indicating that relevant amounts of doxorubicin can be loaded into this platform.

Doxorubicin release from particles exposed to NIR light or simply left at room temperature is displayed in Figure 5A. Particles exposed to NIR light for 3 min released 22.2 ± 1.4 μg doxorubicin/1×10^9 particles. Minimal release was seen from particles that were not exposed to NIR light over the 3 min period, and only 6.6 ± 0.5 μg doxorubicin/1×10^9 particles, or less than 15% of the payload, was released from the particles after 72 h at room temperature, as shown in Figure 5A. Additionally, only 25% of the payload was released when incubated at 37 °C over 48 h, and the presence of serum did not affect this release, indicating minimal diffusional release over time periods longer than required for EPR-mediated tumor uptake of nanoparticles (see the Supporting Information).

In a separate study using doxorubicin-loaded particles, NIR light exposure was cycled on and off over a 9 min period (3 min on, 3 min off, 3 min on). A significant amount of drug was released when the laser was on and negligible release for the 3 min period without laser exposure (Figure 5B), demonstrating the dependence of release kinetics on NIR exposure.

3.5. Drug Delivery to Carcinoma Cells. Fluorescence microscopy was used to analyze the amount of doxorubicin uptake by cells exposed to irradiated and nonirradiated doxorubicin-loaded particles after a 24 h dosing period. Figure 6A−C shows that cells exposed to doxorubicin-loaded particles and NIR light display nearly 2.5 times as much doxorubicin fluorescence per cell compared to cells exposed to non-irradiated particles, indicating that doxorubicin released from these irradiated particles efficiently enters the cells.

To evaluate efficacy of the delivered drug, we assessed cell viability 24 h after particle dosing for the five experimental conditions described above. Figure 6D displays these results. Cells exposed to doxorubicin-loaded particles and NIR light showed almost a 90% decrease in cell viability compared to nontreated controls, whereas when these particles were not exposed to NIR light, but allowed to release doxorubicin via slow passive diffusion, only a 55% decrease in viability was observed. Additionally, cells exposed to hydrogel-coated particles without drug but with NIR light exposure did not show any changes in viability, indicating that the heating generated by these particles alone at this laser intensity and irradiation time was not sufficient to cause cell death. Only about a 20% decrease in cell viability was seen in the free drug control, as the concentration of doxorubicin (~50 nM) is well below the reported IC50 values for CT.26WT cells (~1 μM),[22] suggesting differences in drug uptake depending on the delivery method.

4. DISCUSSION

Successful drug delivery carriers in cancer should meet four basic requirements: (1) retain the drug during circulation, (2) evade the body's defenses, (3) access the tumor site, and (4) release the drug, specifically at the tumor site.[23] The particles developed in this study were designed to retain drug in the poly(NIPAAm-*co*-AAm)-hydrogel coating, access tumor tissue through the EPR effect (as they are synthesized as sub-500 nm particles), and release the drug payload upon NIR exposure. Furthermore, it is hypothesized that the poly(NIPAAm-*co*-AAm)-hydrogel coating will act to stabilize the particles and evade clearance from the bloodstream similarly to the poly(ethylene glycol) (PEG) brushes utilized on many nanoparticle platforms, although further investigation of this aspect is required. Additionally, incorporation of tumor-specific ligands onto particle surfaces is commonly used to improve accumulation of nanoparticles in tumor tissue.[24] The hydrogel coating used in these studies would allow for conjugation of such targeting moieties (proteins, peptides, etc.).

To fabricate hydrogel-coated nanoshells, we grew a thin poly(NIPAAm-*co*-AAm) hydrogel coating onto individual gold−silica nanoshells using SI-ATRP. Similar studies synthesizing hydrogel coatings via SI-ATRP have been reported;[25−27] however, aggregation issues due to interparticle interactions during the growth of the hydrogel coatings and multiple processing steps often lead to low yields.[26,28] To remedy this, Chirra et al. proposed a novel solution in which gold nanoparticles are first stabilized in a flexible hydrogel matrix prior to initiator immobilization and hydrogel growth.[28] After synthesis of the hydrogel coating, the flexible matrix is then dissolved and individual particles may be collected.[28] This scheme served as an inspiration for the synthesis process used in this work, where we utilized Ca^{2+}-alginate hydrogels, which are easily disrupted upon Ca^{2+} chelation, as a temporary matrix.

Analysis by DLS showed that particles increased in size from ~160 nm to over 300 nm with the addition of this coating. Additionally, the hydrodynamic diameter of these particles decreases in response to elevated temperatures and NIR light. It is important to note that DLS measurements are dependent on many factors, including particle geometry and material refractive index, and therefore may not truly represent the particle's real "size", but should allow evaluation of trends between similar materials. A decrease in hydrodynamic diameter (~60 nm) was observed in response to elevated temperatures or NIR light. This reflects extensive collapse of the hydrogel coating, as these modest changes in overall particle size are due to the fact the majority of the particle's volume is made up the incompressible and nonthermally responsive nanoshell.

The poly(NIPAAm-*co*-AAm) coating passivated the particle surface, preventing aggregation under salt conditions as effectively as PEG coatings traditionally used on gold nanoparticle platforms. Furthermore, these particles did not elicit any cytotoxicity against either fibroblasts or hepatic cells in vitro. The chemotherapeutic doxorubicin was loaded into the particles to a concentration of 5×10^7 drug molecules/particle, and ~46% of the payload was released after just 3 min of NIR exposure, whereas less than 15% was released via diffusion over 72 h. This indicates that it should be possible to inject particles and observe minimal drug release over the time required for particle accumulation in the tumor via the EPR effect (typically <24 h), and then trigger rapid delivery of therapeutic doses at the tumor site by exposure to NIR light.

Further analysis showed that this platform can effectively deliver doxorubicin to colon carcinoma cells in vitro. Cells exposed to particles and NIR light displayed nearly 2.5 times as much doxorubicin uptake as cells exposed to particles without

DOI: 10.1021/acsbiomaterials.5b00111
ACS Biomater. Sci. Eng. 2015, 1, 685−692

light, as assessed by fluorescence microscopy. This in turn also resulted in a higher loss in cell viability for cells exposed to drug-loaded particles and NIR light. Drug uptake in cells may also be enhanced by particle heating. Previous studies utilizing gold nanoshells have shown that nanoshell exposure to NIR causes transient increases in membrane permeability of cancer cells.[10,29] As NIR irradiation of this platform causes a release of high concentrations of drug molecules and potentially induces an increase in membrane permeability at the same time, there may be an increased ability for drug molecules to enter the cell, causing increased uptake compared to nonirradiated particles or free drug controls. Current and future efforts are focusing on investigating the in vivo efficacy of these doxorubicin-loaded particles.

5. CONCLUSIONS

The ability to precisely control therapeutic delivery to malignant tissue would undoubtedly improve cancer management by overcoming the limitations of current therapies. The hydrogel-coated particles developed in this work can be loaded with cancer therapeutics such as doxorubicin, and release of the drug is tightly controlled to occur upon exposure to NIR light. Furthermore, delivery from this platform results in increased drug uptake compared to free drug, likely due to platform irradiation causing a transient increase in cell membrane permeability. In fact, under the laser conditions used in these studies, heating alone did not result in any cell death but appeared to increase delivery of the drug into the cells. Ultimately, such a platform could be used to attack tumor tissue using two distinct mechanisms simultaneously: (1) photothermal therapy and (2) delivery of drugs, providing a novel approach to effectively treat cancers when standard treatment modalities are not adequate.

■ ASSOCIATED CONTENT

Supporting Information

The Supporting Information is available free of charge on the ACS Publications website at DOI: 10.1021/acsbiomaterials.5b00111.

Further discussion of batch-to-batch variability, material cytotoxicity, and doxorubicin loading and release (PDF)

■ AUTHOR INFORMATION

Corresponding Author

*E-mail: jennifer.l.west@duke.edu. Tel: 919-660-5458.

Author Contributions

The manuscript was written through contributions of all authors. All authors have given approval to the final version of the manuscript.

Funding

Funding was provided by the NIH (Grants T32EB009379 and U54CA151668).

Notes

The authors declare no competing financial interest.

■ ABBREVIATIONS

EPR, enhanced permeability and retention
NIR, near-infrared
LCST, lower critical solution temperature
NIPAAm, *N*-isopropylacrylamide
AAm, acrylamide
SI-ATRP, surface initiated-atom transfer radical polymerization
OD, optical density

■ REFERENCES

(1) Hirsch, L. R.; Gobin, A. M.; Lowery, A. R.; Tam, F.; Drezek, R. A.; Halas, N. J.; West, J. L. Metal Nanoshells. *Ann. Biomed. Eng.* **2006**, *34*, 15−22.

(2) Shukla, R.; Bansal, V.; Chaudhary, M.; Basu, A.; Bhonde, R. R.; Sastry, M. Biocompatibility of gold nanoparticles and their endocytotic fate inside the cellular compartment: a microscopic overview. *Langmuir* **2005**, *21*, 10644−10654.

(3) Pan, Y.; Neuss, S.; Leifert, A.; Fischler, M.; Wen, F.; Simon, U.; Schmid, G.; Brandau, W.; Jahnen-Dechent, W. Size-dependent cytotoxicity of gold nanoparticles. *Small* **2007**, *3*, 1941−1949.

(4) Gad, S. C.; Sharp, K. L.; Montgomery, C.; Payne, J. D.; Goodrich, G. P. Evaluation of the toxicity of intravenous delivery of auroshell particles (gold-silica nanoshells). *Int. J. Toxicol.* **2012**, *31*, 584−594.

(5) Matsumura, Y.; Maeda, H. A New Concept for Macromolecular Therapeutics in Cancer Chemotherapy: Mechanism of Tumoritropic Accumulation of Proteins and the Antitumor Agent Smancs. *Cancer Res.* **1986**, *46*, 6387−6392.

(6) Weissleder, R. A clearer vision for in vivo imaging. *Nat. Biotechnol.* **2001**, *19*, 316−317.

(7) Day, E. S.; Morton, J. G.; West, J. L. Nanoparticles for thermal cancer therapy. *J. Biomech. Eng.* **2009**, *131*, 074001.

(8) Kelly, K. L.; Coronado, E.; Zhao, L. L.; Schatz, G. C. The Optical Properties of Metal Nanoparticles: The Influence of Size, Shape, and Dielectric Environment. *J. Phys. Chem. B* **2002**, *107*, 668−677.

(9) O'Neal, D. P.; Hirsch, L. R.; Halas, N. J.; Payne, J. D.; West, J. L. Photo-thermal tumor ablation in mice using near infrared-absorbing nanoparticles. *Cancer Lett.* **2004**, *209*, 171−176.

(10) Hirsch, L. R.; Stafford, R. J.; Bankson, J. A.; Sershen, S. R.; Rivera, B.; Price, R. E.; Hazle, J. D.; Halas, N. J.; West, J. L. Nanoshell-mediated near-infrared thermal therapy of tumors under magnetic resonance guidance. *Proc. Natl. Acad. Sci. U. S. A.* **2003**, *100*, 13549−13554.

(11) Sasaki, S.; Kawasaki, H.; Maeda, H. Volume Phase Transition Behavior of N-Isopropylacrylamide Gels as a Function of the Chemical Potential of Water Molecules. *Macromolecules* **1996**, *30*, 1847−1848.

(12) Galaev, I. Y.; Mattiasson, B. 'Smart' polymers and what they could do in biotechnology and medicine. *Trends Biotechnol.* **1999**, *17*, 335−340.

(13) Schild, H. G. Poly(N-isopropylacrylamide): experiment, theory and application. *Prog. Polym. Sci.* **1992**, *17*, 163−249.

(14) Sershen, S. R.; Westcott, S. L.; Halas, N. J.; West, J. L. Temperature-sensitive polymer-nanoshell composites for photothermally modulated drug delivery. *J. Biomed. Mater. Res.* **2000**, *51*, 293−298.

(15) Bikram, M.; Gobin, A. M.; Whitmire, R. E.; West, J. L. Temperature-sensitive hydrogels with SiO2-Au nanoshells for controlled drug delivery. *J. Controlled Release* **2007**, *123*, 219−227.

(16) Strong, L. E.; Dahotre, S. N.; West, J. L. Hydrogel-nanoparticle composites for optically modulated cancer therapeutic delivery. *J. Controlled Release* **2014**, *178*, 63−68.

(17) Kennedy, L. C.; Bickford, L. R.; Lewinski, N. A.; Coughlin, A. J.; Hu, Y.; Day, E. S.; West, J. L.; Drezek, R. A. A New Era for Cancer Treatment: Gold-Nanoparticle-Mediated Thermal Therapies. *Small* **2011**, *7*, 169−183.

(18) Coessens, V.; Pintauer, T.; Matyjaszewski, K. Functional polymers by atom transfer radical polymerization. *Prog. Polym. Sci.* **2001**, *26*, 337−377.

(19) Oldenburg, S. J.; Averitt, R. D.; Westcott, S. L.; Halas, N. J. Nanoengineering of optical resonances. *Chem. Phys. Lett.* **1998**, *288*, 243−247.

(20) Lewinski, N.; Colvin, V.; Drezek, R. Cytotoxicity of nanoparticles. *Small* **2008**, *4*, 26−49.

DOI: 10.1021/acsbiomaterials.5b00111
ACS Biomater. Sci. Eng. 2015, 1, 685−692

(21) MacKay, J. A.; Chen, M.; McDaniel, J. R.; Liu, W.; Simnick, A. J.; Chilkoti, A. Self-assembling chimeric polypeptide-doxorubicin conjugate nanoparticles that abolish tumours after a single injection. *Nat. Mater.* **2009**, *8*, 993−999.
(22) Lee, J.-Y.; Choi, Y.-S.; Suh, J.-S.; Kwon, Y.-M.; Yang, V. C.; Lee, S.-J.; Chung, C.-P.; Park, Y.-J. Cell-penetrating chitosan/doxorubicin/TAT conjugates for efficient cancer therapy. *Int. J. Cancer* **2011**, *128*, 2470−2480.
(23) Needham, D. Materials Engineering of Lipid Bilayers for Drug Carrier Performance. *MRS Bull.* **1999**, *24*, 32−41.
(24) Dong, X.; Mumper, R. J. Nanomedicinal strategies to treat multidrug-resistant tumors: current progress. *Nanomedicine* **2010**, *5*, 597−615.
(25) Li, G. F.; Fan, J. D.; Jiang, R.; Gao, Y. Cross-linking the linear polymeric chains in the ATRP synthesis of iron oxide/polystyrene core/shell nanoparticles. *Chem. Mater.* **2004**, *16*, 1835−1837.
(26) Li, D. X.; He, Q.; Cui, Y.; Wang, K. W.; Zhang, X. M.; Li, J. B. Thermosensitive copolymer networks modify gold nanoparticles for nanocomposite entrapment. *Chem. - Eur. J.* **2007**, *13*, 2224−2229.
(27) Dong, H. C.; Zhu, M. Z.; Yoon, J. A.; Gao, H. F.; Jin, R. C.; Matyjaszewski, K. One-pot synthesis of robust core/shell gold nanoparticles. *J. Am. Chem. Soc.* **2008**, *130*, 12852−12853.
(28) Chirra, H. D.; Spencer, D.; Hilt, J. Z. Isolate, functionalize, and release: the ISOFURE platform for the functionalization of nanoparticles. *J. Nanopart. Res.* **2012**, *14*, 1−8.
(29) Day, E. S.; Bickford, L. R.; Slater, J. H.; Riggall, N. S.; Drezek, R. A.; West, J. L. Antibody-conjugated gold-gold sulfide nanoparticles as multifunctional agents for imaging and therapy of breast cancer. *Int. J. Nanomed.* **2010**, *5*, 445−454.

DOI: 10.1021/acsbiomaterials.5b00111
ACS Biomater. Sci. Eng. 2015, 1, 685−692